# Self-Promoted Cellular Uptake of Peptide/DNA Transfection Complexes†

Lydia Prongidi-Fix,‡ Masae Sugawara,‡ Philippe Bertani,‡ Jesus Raya,‡ Christian Leborgne,§ Antoine Kichler,§ and Burkhard Bechinger*,‡

*Université Louis Pasteur/CNRS, UMR 7177, Institut de Chimie de Strasbourg, 4, rue Blaise Pascal, 67070 Strasbourg, France, and Généthon−Centre National de la Recherche Scientifique, UMR 8115, 1 Rue de l'Internationale, F-91002 Evry, France*

*Received April 24, 2007; Revised Manuscript Received June 20, 2007*

ABSTRACT: The designed α-helical amphipathic peptide LAH4 assembles several properties, which makes it an interesting candidate as a gene-delivery vehicle. Besides being short and soluble in aqueous solutions, LAH4 presents cationic residues, which allow for efficient complexation of DNA. In addition, this peptide is poorly hemolytic at neutral pH, while it is able to destabilize biological membranes in acidic conditions. In this study, the structure of the peptide/DNA transfection complex was examined by circular dichroism and solid-state nuclear magnetic resonance spectroscopies and the thermodynamics of its formation and disassembly was monitored in a quantitative manner as a function of pH by isothermal titration calorimetry. Notably, the number of peptides within the complex considerably decreases upon acidification of the medium. This observation has direct and important consequences for the mechanism of action because the acidification of the endosome results in high local concentrations of free peptide in this organelle. Thus, these peptides become available to interact with the endosomal membranes and thereby responsible for the delivery of the transfection complex to the cytoplasm. When these data are taken together, they indicate a dual role of the peptide during the transfection process, namely, DNA complexation and membrane permeabilization.

Recombinant viruses are the most studied vectors to transfer DNA into cells, and they form the basis of the vast majority of ongoing clinical trials (*1*). Furthermore, our growing knowledge of how these biological vectors function has permitted the development of gene-delivery systems made of greatly simplified components that mimic the advantageous aspects of viral transfection without its apparent side effects. Increasing the efficiency and reducing the cytotoxicity of gene-delivery systems remain major challenges but offer high benefits for basic research, RNA interference, and gene therapy.

Nonviral gene delivery has been performed using a variety of compounds of unrelated structure, such as dendrimers (*2*), polylysine conjugates (*3*), linear and branched polycations (*4*, *5*), block copolymers (*6*), cationic lipids (*7*, *8*), and peptides (*9*, *10*). Among these compounds, synthetic peptide-based gene delivery is the least explored, although it has great biotechnological potential. Indeed, in contrast to most polymers, key parameters, such as product identification, large-scale production and quality control, are possible. Peptides were initially used as cell-targeting moieties (*11*), membrane-destabilizing agents (*12*, *13*), or nuclear-localization elements (*14*). However, cationic peptides are of particular interest because they can combine DNA condensation with membrane-destabilizing capabilities. To our knowledge, KALA was the first efficient synthetic transfection peptide (*9*), a tetrameric repeat that was later improved by replacing the lysines by arginines (*10*). Furthermore, several peptides of the LAH4 family, which we have investigated in this work, have proven to be efficient transfection agents (*15*). We will illustrate that they use a mechanism of vectorization quite different from other known transfection agents, when at the same time, they show low cytotoxicity and high bacteriotoxic activity (*16*). The parent peptide (LAH4)[1] with the sequence KKALL ALALH HLAHL ALHLA LALKK A was initially designed as a model peptide to study the interaction contributions that determine the membrane topology and the membrane-disrupting properties of some α-helical amphipathic peptides, including the antibiotics magainins, cecropins, and the human peptide LL-37 (*17*−*19*). The helical wheel projection shows that LAH4 is characterized by the separation of polar and hydrophobic residues at opposite helical surfaces (Figure 1). Whereas the cationic charge at physiologic pH confers nucleic-acid-condensating properties in aqueous solution (*20*), the hydrophobic face of the peptide allows for efficient membrane interactions. In contrast to previous studies, where the interaction of LAH4 with membranes was investigated (*16*, *21*), the present investigation focuses on biophysical parameters of the LAH4/DNA transfection complexes, such as

† This work has been supported by Grant TG 0411 from Vaincre La Mucoviscidose. In particular, the Ph.D. fellowship to L.P.-F. was essential and has allowed us to pursue this work.

* To whom correspondence should be addressed: Faculté de Chimie, 4, rue Blaise Pascal, 67070 Strasbourg, France. Telephone: +33-3-90-24-51-50. Fax: +33-3-90-24-51-51. E-mail: bechinger@chimie.u-strasbg.fr.

‡ Université Louis Pasteur/CNRS.

§ Généthon−Centre National de la Recherche Scientifique.

[1] Abbreviations: CD, circular dichroism; HPLC, high-performance liquid chromatography; ITC, isothermal titration calorimetry; LAH4, peptide with the sequence KKALL ALALH HLAHL ALHLA LALKK A; MALDI−MS, matrix-assisted laser desorption/ionization mass spectrometry; MAS, magic angle sample spinning; NMR, nuclear magnetic resonance.

10.1021/bi700766j CCC: $37.00 
Published on Web 09/12/2007

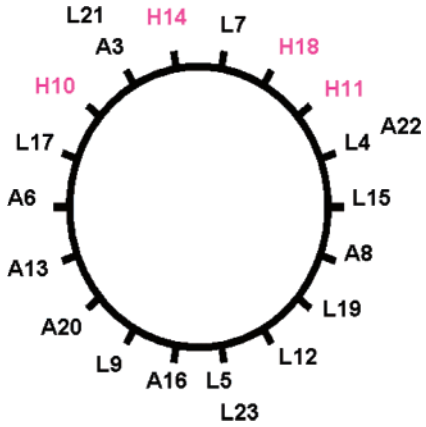


FIGURE 1: Edmundson helical wheel diagram of the core region of LAH4. Because of the potentially flexible structure of lysine side chains and the polypeptide terminal residues, K1−K2 and K24−K25−A26 are not shown.

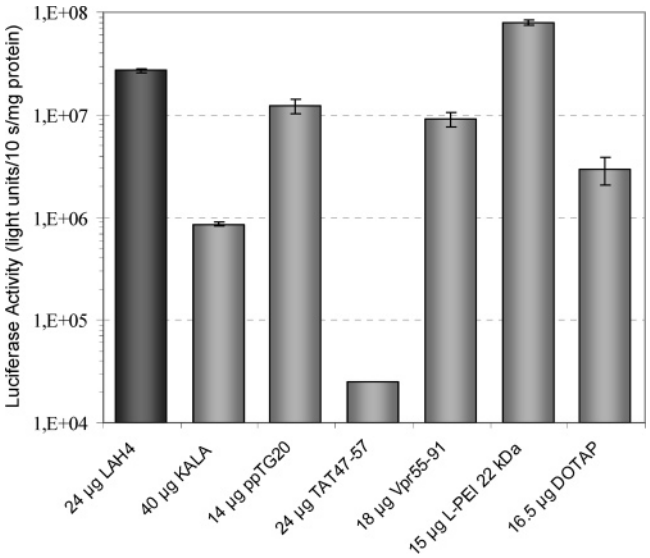


FIGURE 2: Transfection efficiency of various cationic compounds [the monocationic lipid DOTAP (*39*), the linear polymer PEI of 22 kDa (*40*), and the cationic peptides KALA (*9*), TAT47-57 (*29*), ppTG20 (*30*), Vpr55-91 (*59*), and LAH4] on human hepatocarcinoma cells (HepG2) are compared to each other. The best mixture is shown for each compound. The amounts of cationic agent used are indicated in the figure (as $\mu$g/4 $\mu$g of DNA. The error bar for the TAT peptide is too small to be visible in this logarithmic representation.

structure, charge, and composition, as well as the resulting characteristics of the disassembly process.

Isothermal titration calorimetry (ITC) has been used successfully in previous studies to elucidate peptide−DNA (*22*−*24*) or peptide−membrane association (*25*, *26*). It has also been used to better understand the association of DNA with cationic lipids used in transfection experiments (*27*, *28*). Here, we characterize for the first time the composition, association, and disassembly of a peptide transfection vector with DNA as a function of environmental conditions. This quantitative analysis is indicative of how the transfection complex is released into the cytoplasm. Furthermore, circular dichroism (CD) and solid-state nuclear magnetic resonance (NMR) spectroscopies provide complementary structural information on the complex. The ensemble of results leads to a structural and functional description of the multiple roles of the LAH4 peptide during transfection. Importantly, the resulting model provides a simple concept for the design of novel transfection peptides or the interpretation of "mutagenesis" data of such transfection peptides.

## MATERIALS AND METHODS

*Materials.* All chemicals were purchased at the highest purity from commercial sources.

*Peptide Synthesis.* The peptide (KKALL ALALH HLAHL ALHLA LALKK A) LAH4 was synthesized by solid-phase peptide synthesis on a Millipore 9050 automatic peptide synthesizer by using standard synthesis cycles. A 4-fold excess of Fmoc-protected amino acids (Calbiochem, Läufelfingen, Switzerland) was used during chain elongation. A $^{13}C_{\beta}$-labeled Fmoc-protected alanine analogue (Calbiochem, Läufelfingen, Switzerland) was incorporated at either position 6 or 13, respectively (underlined in the sequence shown above). After cleavage from the resin with trifluoroacetic acid, the identity and purity of the peptides was verified using matrix-assisted laser desorption/ionization mass spectrometry (MALDI−MS) and reverse-phase high-performance liquid chromatography (HPLC). The HPLC chromatograms were recorded at 214 nm using an acetonitrile/water gradient in the presence of 0.1% trifluoroacetic acid (TFA).

The other peptides KALA (*9*) (WEAKLAKALAKALA-KHLAKALAKALKA CEA; Synt:em, Nimes, France), TAT47-57 (*29*) (YGRKKRRQRRR, Bachem, Weil-am-Rhein, Germany), ppTG20 (*30*) (GLFRALLRLLRSLWR-LLLRA; Neosystem, Strasbourg, France), and Vpr55-91 (*31*) (TGVEALIRILQQLLFIHFRIGCRHSRIGIIQQ RRTRN, Synt:em) were from the commercial sources indicated.

*Test of Transfection Efficiencies.* DNA was purified using the Plasmid Mega Kit (Qiagen, Courtaboeuf, France). The purity of the DNA was checked by measuring the $A_{260}/A_{280}$ ratio (which was around 1.8) and by agarose gel electrophoresis. The transfection efficiencies were tested by mixing increasing amounts of transfection agent with a constant amount of reporter plasmid (4 $\mu$g of CMV-Luc per duplicate). The complexes were incubated for 3 h in serum-free medium, with cells placed in 24-well plates the day before (250 000 cells/well). The luciferase activity was measured 30 h post-transfection as described in ref *32*. The luciferase background was subtracted from each value, and the protein content of the transfected cells was measured by Bradford dye-binding using the BioRad protein assay. The transfection efficiency is expressed as total light units $(10\ s)^{-1}$ $(mg\ of\ protein)^{-1}$, and the average of duplicates is shown. Only the best formulation for each compound is shown in Figure 2.

*Sample Preparation and Proton-Decoupled $^{13}C$ CP/MAS NMR.* Dry powders of LAH4 peptide, salmon sperm low-molecular-weight DNA (Fluka, Buchs, Switzerland), or complexes thereof were inserted into 4 mm MAS rotors. For complex formation, LAH4 peptide and DNA were first dissolved in a minimum amount of water, mixed at the ratio of 1.2/1 (wt/wt), and lyophilized.

To record proton-decoupled solid-state NMR spectra, a commercial double-resonance probe operating on a 11.7 T Bruker Avance spectrometer was used. Typical acquisition parameters of the cross-polarization sequence (*33*) were the following: 5 s recycle delay; $^1H$ $B_1$ field, 72 kHz (during preparation, cross-polarization and decoupling); $^{13}C$ $B_1$ field, 62 kHz, and spinal 64 proton-decoupling during acquisition;

number of scans, 10 000. The cross-polarization contact time of 0.5 ms was optimal for the imidazonium resonances. Samples were spun at a 10 kHz MAS rate. All experiments were performed at ambient temperature. An exponential apodization function corresponding to a line broadening of 50 Hz was applied before Fourier transformation. The spectra were referenced relative to solid adamantane (38.2 ppm) and assigned using literature data (*34*−*37*).

*Circular Dichroism.* For CD measurements, peptide and DNA were dissolved in 10 mM phosphate buffer or phosphate-buffered saline (PBS, Fluka) at pH 7.5 or 5.5, respectively. The LAH4 samples were prepared at concentrations of 0.2 mg/mL for use in a cell with a 1 mm path length, corresponding to a mean residual concentration of 1.57 mM or of 0.05 mg/mL (0.392 mM) for a two-compartment cell with a 2 × 4.25 mm optical path length (Helma France, Paris). The DNA concentration was fixed at 0.044 mg/mL (1 mm cell) and 0.011 mg/mL (two-compartment cell), respectively.

CD spectra of LAH4 and its complex with DNA were measured on a JASCO J-810 dichrometer using a sweep width of 190−260 nm, a scan speed of 20 nm/min, and 0.2 nm step resolution. For each sample, two spectral scans were accumulated. All spectra were converted to molar ellipticity units by using LAH4 mean residual concentrations. Secondary-structural elements of the peptide were estimated by using the CDSSTR program in the CDPro package (*38*). The normalized root-mean-square difference (NRMSD) values were typically around 0.05, with a value $<0.1$ being indicative of a good fit of the spectrum.

*Isothermal Titration Calorimetry.* ITC was performed using a VP-ITC instrument with a cell volume of 1.4192 mL (MicroCal, Northampton, MA). The peptide and the salmon sperm low-molecular-weight DNA (Fluka, Buchs, Switzerland; ≤5% protein; $A_{260}/A_{280} \sim 1.4$) were dissolved in phosphate saline buffer (137 mM NaCl, 2.7 mM KCl, 10 mM $Na_2HPO_4$, and 2 mM $KH_2PO_4$) at pH 7.5 or 5.5, respectively. Care was taken to prepare the DNA and peptide solutions from the same batch of buffer to minimize mixing artifacts. All solutions were degassed under vacuum prior to use. At 240 s intervals, 8 μL of a 1 mM peptide stock solution was injected into a solution of 0.5 μM DNA and the heat of association was measured. The stirring rate was 300 rpm. The starting solutions in the calorimeter cell and in the syringe were kept at the same temperature (288, 298, or 308 K, respectively). Control experiments were carried out under identical experimental conditions by injecting the peptide into PBS or by injecting PBS into DNA solutions. The results of the titration experiments were analyzed using the MicroCal Origin software of the ITC instruments.

*Centrifugation Assay.* Solutions of LAH4 peptide and *Escherichia coli* genomic DNA were prepared in PBS buffer at pH 7.5, mixed to yield 9 μg of LAH4 and 3 μg of DNA in 500 μL, incubated for 20 min at room temperature, and centrifuged for 10 min at 14000*g*. The supernatant of this first centrifugation was kept for UV spectrometry measurements, while the pellet was resuspended in PBS at different pH values. The suspensions were incubated at room temperature during 1 h and then centrifuged for 10 min at 14000*g*. The supernatants of both centrifugations were tested UV spectrophotometrically in the range of 190−300 nm using a UVIKON 922 spectrometer (BIO-TEK Kontron Instruments, Munich, Germany). The optical densities of the supernatants showed no trace of DNA in solution. The LAH4 concentrations of the supernatants were calculated from the optical densities at 214 nm. All steps were performed at room temperature.

*DNA Retardation Assay.* DNA binding was studied by means of an agarose gel retardation assay. Briefly, plasmid DNA (1 μg) and increasing amounts of LAH4 (from 1 to 3 μg) were each diluted in 25 μL of either a citric acid buffer at pH 5, a Hepes-buffered saline (HBS) at pH 6 or 6.5, or a PBS buffer at pH 7.5. DNA and the peptide were then mixed, and after a period of 15 min, samples (20 μL) were electrophoresed through a 1% agarose gel using Tris−borate−ethylenediaminetetraacetic acid (EDTA) buffer at pH 7.4. The DNA was visualized after ethidium bromide (EtBr) staining.

## RESULTS

*Transfection Efficiency of LAH4/DNA Complexes.* In a first step, we have compared the transfection efficiency of LAH4 to other known DNA transfection agents, including cationic lipids (*39*), polymers (*40*), and peptides (*9*, *30*, *41*), as well as to the cell-penetrating TAT peptide (*29*). Figure 2 as well as results shown in ref *15* indicate that the activity of LAH4 compares very well with other transfection compounds. These results, together with the fact that LAH4 exhibits low cytotoxicity (*15*), underscores the high potential of this peptide.

*CD Spectroscopy.* To follow the conformational changes of the peptide during complex formation, CD spectroscopy was performed. The spectra shown in Figure 3 were acquired as a function of pH as well as in the absence and presence of DNA. Control experiments indicate that the dichroism of DNA can be neglected in the spectral region $<260$ nm (data not shown), and the spectra are therefore directly indicative of the polypeptide secondary structures.

The quantitative analysis of the CD spectral line shapes shows that, in the absence of DNA, LAH4 is predominantly random coil at low pH (5% α helix) but adopts 41% helicity when the pH is increased (Figure 3A). This is in excellent agreement with previous data (*16*). The data are suggestive that, at neutral pH and in analogy to the concentration-dependent formation of helical aggregates of melittin (*42*, *43*) or LL-37 (*19*, *44*), LAH4 also associates into small oligomers for the peptides to mutually cover their hydrophobic surfaces. This oligomerization is concomitant with the formation of amphipathic α-helical structures.

The CD spectra of LAH4 recorded in the presence of DNA show the characteristic minima near 208 and 222 nm; again, this is indicative of an α-helical secondary structure. Whereas at pH 7.5, the helicity of LAH4 is maintained upon association with DNA (41%), it increases considerably at pH 5.5 from 5% when free in solution to reach 35% upon the addition of DNA. Notably, these values reflect the average helix content of peptides associated with the complex and peptides that remain in solution.

Figure 3B shows the results of a titration experiment where LAH4 was added to a DNA solution in a stepwise manner. At pH 7.5, the changes are small, indicating that the secondary structure of LAH4 remains similar at all LAH4/DNA molar ratios tested. However, at pH 5.5, the LAH4

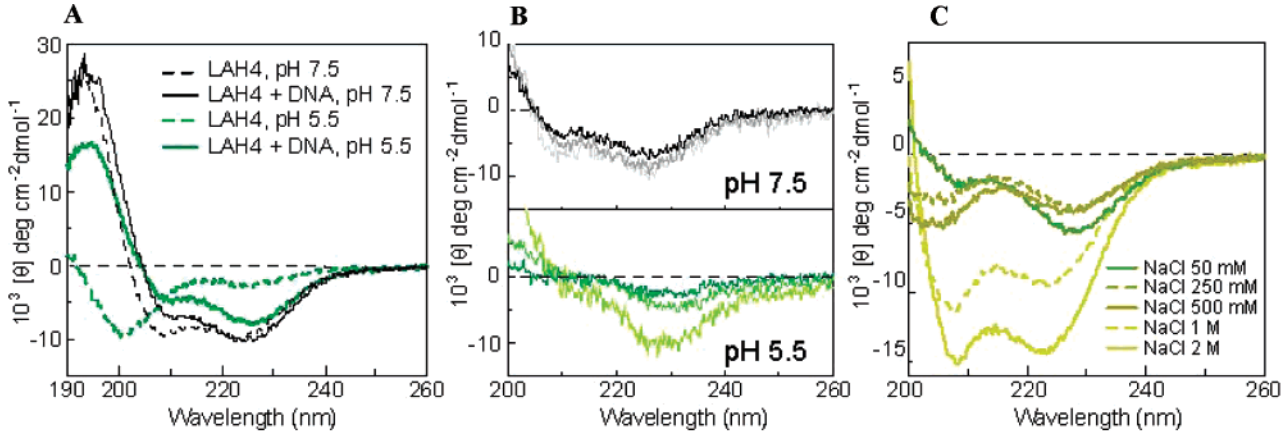


FIGURE 3: CD spectra of (A) LAH4 with or without DNA (300 bp) in 10 mM phosphate buffer at the indicated pH values. The peptide concentration was 0.05 mg/mL. After the addition of DNA (0.11 mg/mL), the molar ratio of LAH4/DNA was 240. (B) Titration of increasing amounts of LAH4 into a 0.25 $\mu$M DNA solution at the pH values indicated. The molar ratio of LAH4/DNA is equal to 72 (light gray line, light green line), 121 (gray line, green line), and 168 (black line, dark green line). At pH 5.5, the LAH4/DNA complex precipitated within the quartz cell, thereby displaying increased light scattering. It should be noted that the concentrations of the transfection complex are increased when compared to A. (C) Ionic force inducing spectral changes of the LAH4/DNA complex at pH 5.5. The sample concentrations were fixed at 0.2 mg/mL LAH4 and 0.044 mg/mL DNA (as in B) to respect the molar ratio of LAH4/DNA equal to 240.

signal was lost when the LAH4/DNA molar ratio was increased. In parallel, the optical density of the sample augments (data not shown), indicating that particles several 100 nm in size are formed that scatter the incident light beam. Subsequently, the particles precipitate and are thereby removed from the light path. Notably, this latter effect is reduced by increasing the salt concentration (Figure 3C).

*Magic Angle Spinning Solid-State NMR Spectroscopy.* The secondary structure analysis by CD spectroscopy works well for polypeptides or LAH4/DNA complexes that, in aqueous solution, remain dissolved or dispersed as small assemblies. In contrast, the method fails when large macromolecular structures form. Therefore, we studied the LAH4/DNA transfection complexes by proton-decoupled $^{13}$C solid-state NMR spectroscopy. Numerous proteins and peptides have been investigated using NMR techniques, and correlations have been established between the CO, $C_\alpha$, and $C_\beta$ $^{13}$C chemical shifts and the secondary structure of the polypeptide chain (*45*, *46*). For example, the spectra of α-helical domains exhibit CO intensities at 176 ± 1 ppm, whereas the carbonyls of pleated sheet structures resonate at 171 ± 1.5 ppm (*34*, *45*, *46*). Similarly the chemical-shift values of the Ala-$C_\beta$ intensities occur at 15.5 ± 3 or 21 ± 1 ppm for α-helical and $\beta$-sheet conformations, respectively (*34*, *45*−*48*).

Proton-decoupled $^{13}$C solid-state NMR spectra of LAH4, DNA, and the complex are shown in Figure 4, including the assignments of resonances that have been performed according to literature data (*34*−*37*). Figure 4A indicates that LAH4 exhibits a well-defined peak intensity at 15.6 ppm, comprising the $C_\beta$ chemical shift of eight alanines of the LAH4 sequence that add up to a maximum, while the signal intensities of the carbonyl carbons are characterized by an unresolved line situated at 176.1 ppm. We also prepared two peptides, where the $C_\beta$ carbons of either alanine-6 or alanine-13 were selectively enriched with $^{13}$C, and these sites exhibit resonances at 15.1 and 15.2 ppm, respectively. These data indicate that the core region of the LAH4 peptide and the backbone of residues 6 and 13, in particular, adopt predominantly α-helical structures in the peptide lyophilizate.

Furthermore, the proton-decoupled $^{13}$C MAS NMR spectra of low-molecular-weight DNA at natural isotopic abundance was recorded in the solid state (Figure 4B), and the peaks were assigned using literature data (*37*, *49*).

Figure 4C shows the $^{13}$C CP/MAS spectrum of the LAH4/DNA complex. When compared to a spectrum obtained by the summation of the individual recordings from the peptide and DNA (parts A and B of Figure 4), the chemical-shift peak positions of the complex remain largely unaltered, although some subtle changes, such as line broadening, are also observed. The obvious similarity of the $^{13}$C chemical shifts obtained from the peptide alone (Figure 4A) or within the transfection complex (Figure 4C) indicates that its predominantly α-helical character is preserved during its association with DNA. This is confirmed by NMR spectra obtained from single-site-labeled peptides, which exhibit $^{13}C_\beta$ resonances at 15.6 ppm (Ala 6) and 15.9 ppm (Ala 13) as well as CO peaks at 176.2 ppm (not shown). These values are very similar to those observed before the complex formation.

*Composition of the Transfection Complex as a Function of pH.* As the imidazole groups of the histidine residues become protonated at acidic pH, we asked whether the quantity of peptides in the transfection complexes changes with pH. To address this point, we determined, in a first experiment, the amount of peptide required to prevent penetration of plasmid DNA into the agarose mesh and migration of the complex toward the cathode during gel electrophoresis. The results of the gel-shift experiments indicate that, for complexes prepared at neutral pH, a w/w ratio of approximately 2.8 (LAH4/plasmid DNA) is required for the formation of large complexes and the concomitant inhibition of plasmid DNA migration through the gel (Figure 5). This corresponds to a molar ratio of 0.6 peptides/bp. When DNA complexes were generated at pH 5, the amount of LAH4 needed for complete retardation is only about half of this value. This observation is highly relevant to the transfection mechanism because the complexes are formed at neutral pH but are exposed to the acidic environment of endosomes during the transfection process (*15*).

Therefore, we tested if association is reversible and if the complexes formed at high pH release significant amounts of peptide when the pH is decreased. A centrifugation assay

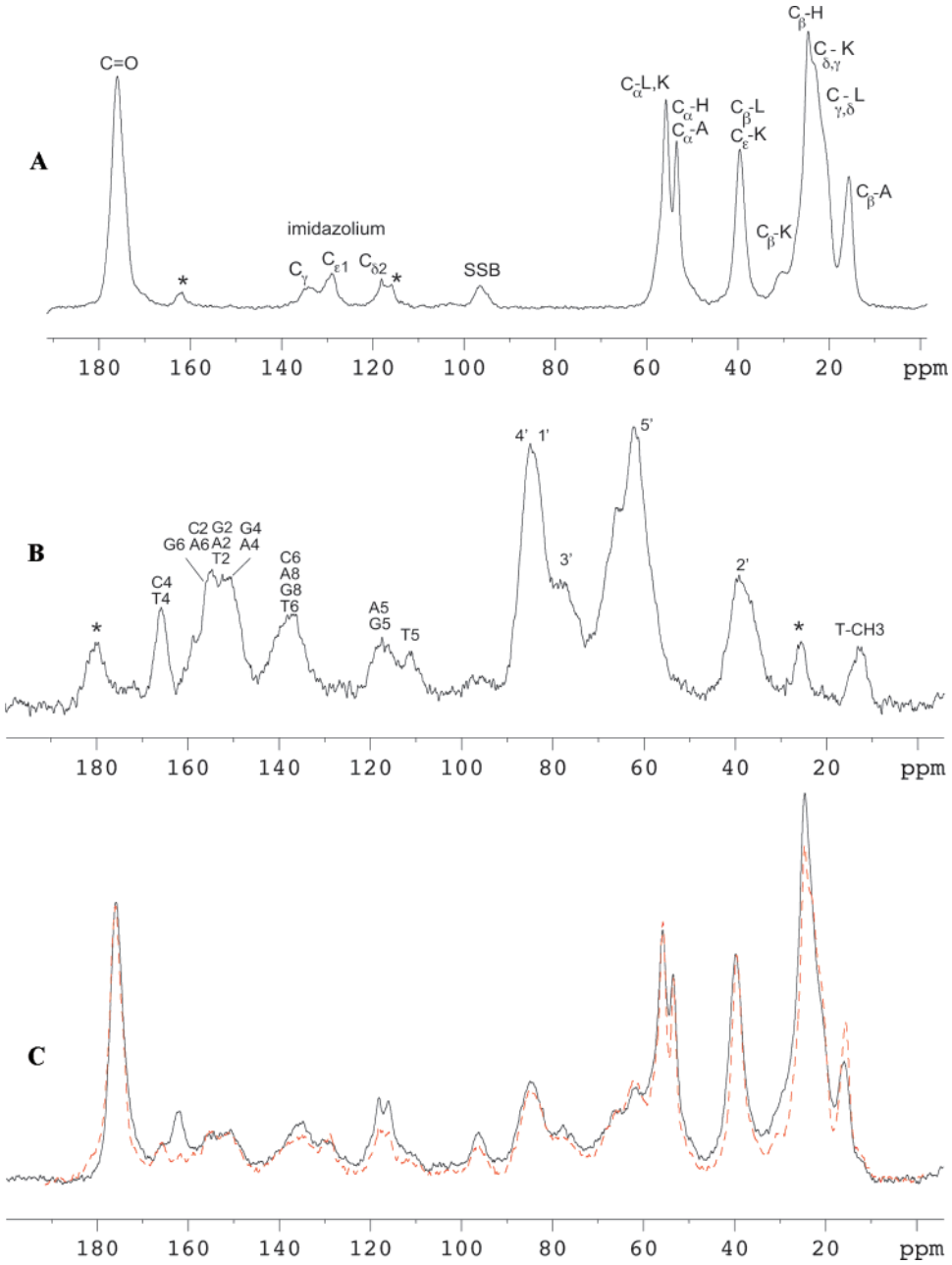


FIGURE 4: Proton-decoupled $^{13}C$ MAS solid-state NMR spectra recorded at ambient temperature. Lyophilized powders of (A) the LAH4 peptide, (B) sonicated salmon sperm DNA (average size of 4 kbp), and (C) a complex of LAH4 and DNA (solid line). The sum of spectra A and B is also shown for a comparison (red dashed line). SSB = spinning side band. (*) Resonances from $CF_3COOH$ (spectrum A) or Tris−EDTA buffer (spectrum B), respectively.

was designed in which complexes are formed at pH 7.4 from LAH4 and large DNA fragments under conditions where the binding sites on the DNA strands are saturated by peptides. The complexes are precipitated, which allows us to remove the excess peptide, which remains in solution. In a next step, the complexes were resuspended in buffer of variable pH, the complexes were precipitated, and the amount of peptide that is released into the supernatant was monitored in a quantitative fashion. The resulting composition of the complexes can thus be evaluated as a function of pH (Figure 6). The centrifugation assay confirms a significantly reduced number of binding sites on the DNA when the pH is decreased from 7.5 to 5.5. Whereas in the centrifugation assay, the decrease is stepwise when the p*K* values of the histidines are reached (Figure 6); a more continuous change is observed in the gel-shift experiments (Figure 5). This is probably due to a better definition of the environmental pH in the presence of the bulk solutions of the centrifugation assay.

*Calorimetric Analysis of LAH4/DNA Interactions.* Having established that the pH-dependent changes in the composition of the transfection complexes are reversible, ITC was used to investigate the equilibrium thermodynamics of complex formation as a function of pH. In these experiments, the heat changes are directly measured upon the addition of small volumes of concentrated LAH4 to the reaction cell containing the DNA solution (Figure 7). Integration yields the calorimetric binding enthalpy ($\Delta H$) as a function of the peptide concentration. In control experiments, the enthalpy of the LAH4 dilution was determined (*25*, *50*) and subtracted from

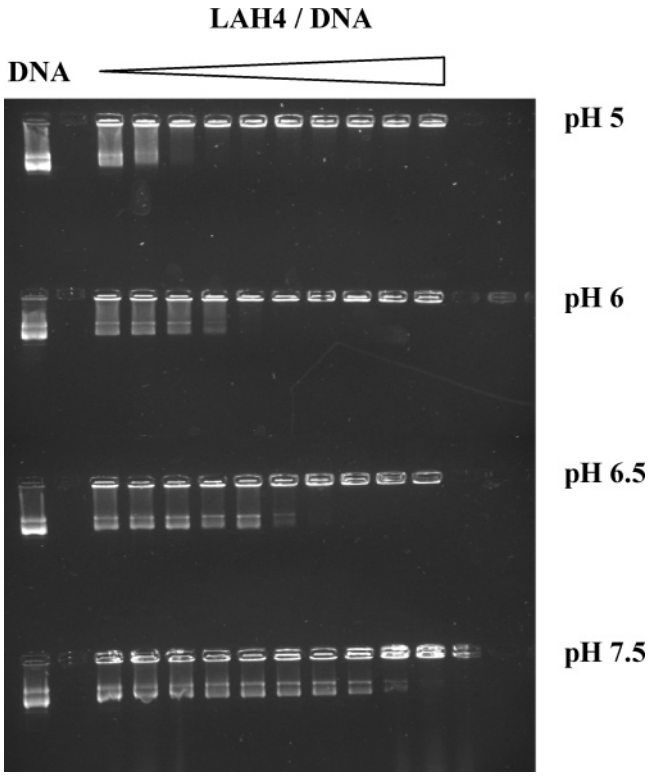


FIGURE 5: Gel retardation experiment of LAH4/DNA mixtures performed at pH 5, 6, 6.5, and 7.5, respectively. The DNA-binding assay was performed as described in the Materials and Methods. The following amounts of LAH4 were used with 1 $\mu$g of DNA (from left to right): 1, 1.2, 1.4, 1.6, 1.8, 2.0, 2.2, 2.4, 2.8, and 3.0 $\mu$g.

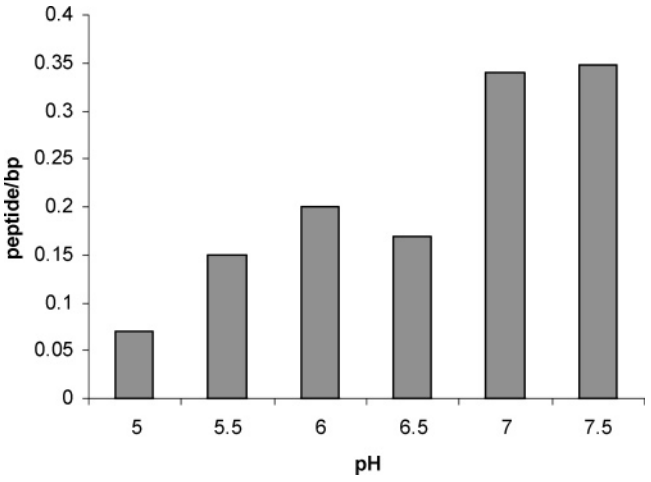


FIGURE 6: Composition of the precipitated transfection complexes after incubation in PBS buffer of variable pH.

the total change in enthalpy because of the formation of the LAH4/DNA complex. In contrast, DNA dilution results in negligible heat changes under all conditions tested.

The resulting titration curves were analyzed assuming a single type of binding site, directly providing both the association constant ($K$) and the number of peptides per 300 bp DNA fragment ($N$). The free-energy change ($\Delta G$) and the entropy change ($\Delta S$) during complex formation are obtained using standard thermodynamic relationships. Titrations were performed in the temperature range of 15−35 °C, in which both the peptide and the DNA are thought to undergo only limited conformational changes (*22*, *24*).

The thermodynamic parameters thus obtained at 298 K at two pH values are shown in Table 1. The values of $\Delta G$ are negative under all conditions tested, favoring association, and in all cases, this association process is entropy-driven. However, the reaction is exothermic at pH 7.5 and endothermic at pH 5.5. This strong pH dependence is indicative of significant differences when the interaction contributions at neutral and low pH are compared with each other. Although the enthalpy and entropy changes during association vary considerably under the different conditions tested, this variation is counter-directional, such that the free-energy values ($\Delta G$) remain roughly constant (Table 1). Such entropy−enthalpy compensation has been described for other biological systems and is discussed in ref *51*. The ITC data confirm in a quantitative manner that there are about twice as many binding sites on the DNA at pH 7.5 than at pH 5.5 at room temperature and at millimolar concentrations of the peptide.

## DISCUSSION

Transfection complexes composed of the amphipathic peptide LAH4 and DNA were formed, and their size and structure were investigated by a variety of biophysical methods, including $\zeta$-potential measurements (*52*) and CD and solid-state NMR spectroscopies. The data indicate that the peptide maintains its strong propensity to form $\alpha$-helical structures in the presence of DNA (Figures 3 and 4) as well as in membrane environments and in solution at neutral pH (*16*). The best transfection efficiency is obtained when LAH4 is mixed with DNA at a ratio of 6:1 (wt/wt, or 1.42 peptides/bp); i.e., the number of lysine residues exceeds by far the number of phosphates (*15*). Although our data indicate that not all of the peptide that has initially been added for complex formation also stably associates with DNA (Figure 5), it is not surprising that a large complex is formed, exhibiting an overall positive $\zeta$ potential of 10 mV in the presence of 150 mM NaCl (*52*). The zetasizer measurements also indicate that, at pH 7, the complexes reach several micrometers in diameter when generated in 150 mM salt solutions, while they are in the 100 nm range when assembled in a salt-free solution (5% glucose). Interestingly, such a salt-dependent aggregation was also described for other transfection agents, in particular, for the cationic polymer polyethylenimine (*53*). At the present time, the structural details of the transfection complex, such as the interaction surface between DNA and peptide, are unknown because classical structural techniques are hampered by the large size and noncrystalline nature of the complexes.

In a next step, gel-shift experiments, a centrifugation assay, and ITC were used to analyze in quantitative detail the thermodynamic contributions during complex formation as well as the stoichiometry at low and neutral pH (Table 1). These experiments indicate that, at neutral pH, about one peptide/2 base pairs reversibly associates with DNA and the thermodynamic signature, with the enthalpic contribution close to zero, suggests that peptide−DNA association is governed by electrostatic interactions (*22*, *25*, *27*). When the transfection complexes are formed in the presence of excess amounts of peptide [ratio of 6:1 (wt/wt) or LAH4/bp of 1.42 (mol/mol)], it is ensured that, at pH 7.5, most, if not all, of the available binding sites on the DNA molecules are occupied. The data also indicate that the capacity of DNA

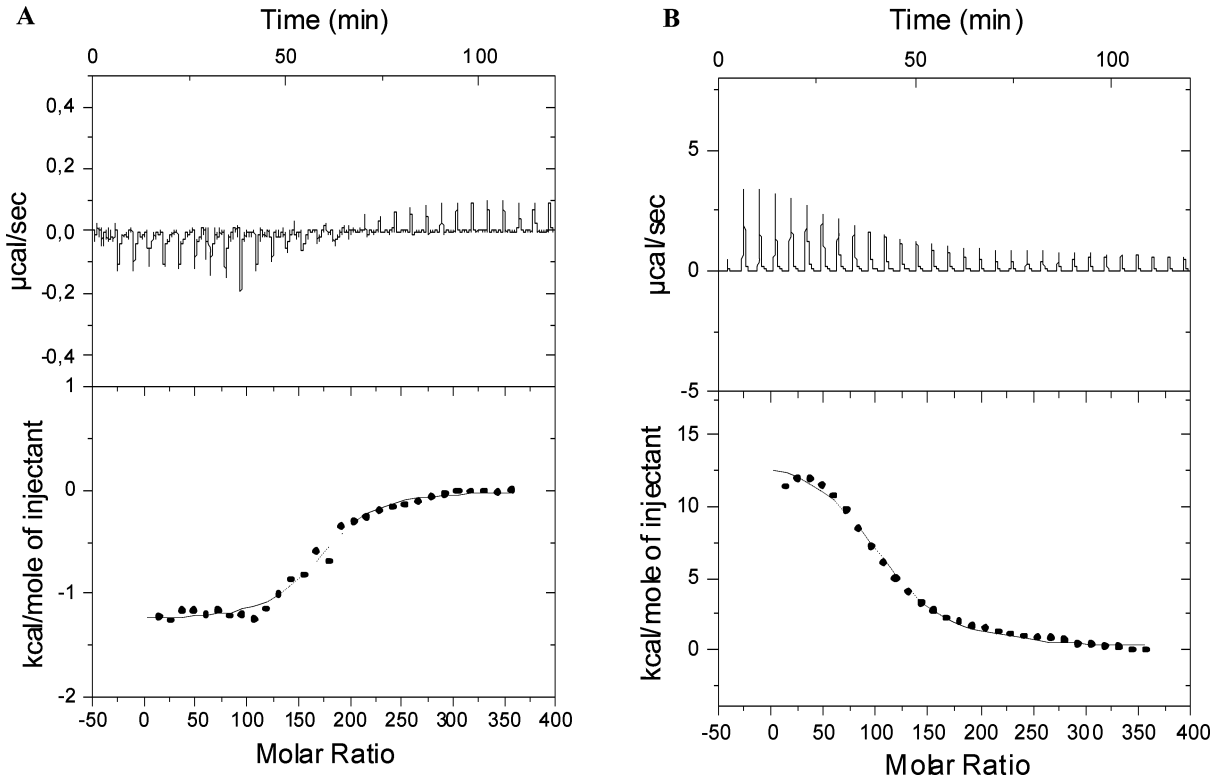


FIGURE 7: Isothermal titration of low-molecular-weight salmon sperm DNA (ca. 300 bp) with the LAH4 peptide. (a) pH 7.5 and (b) pH 5. Titration of 0.5 $\mu$M DNA with 1 mM LAH4 (upper panel). The peptide was added in 40 aliquots of 8 $\mu$L each, in phosphate-buffered saline at 25 °C. Integration of these peaks and subtraction of the heats of dilution produces the binding isotherm shown in the lower panel. The points are fitted to a model for a single type and independent binding sites.

Table 1: ITC Thermodynamic Parameters Describing the Interaction of LAH4 with DNA as a Function of pH[a]

| temp (K) | pH | concn (mM) | $\Delta H$ (kJ/mol) | $T\Delta S$ (kJ/mol) | $\Delta G$ (kJ/mol) | $K_a$ ($\mu M^{-1}$) | $N$ | $n$ |
|---|---|---|---|---|---|---|---|---|
| 298 | 7.5 | 0.5−1 | $-6 \pm 1$ | $25 \pm 2$ | $-31 \pm 2$ | $30 \pm 16$ | $148 \pm 39$ | 4 |
| 298 | 5.5 | 0.5−1 | $51 \pm 9$ | $82 \pm 8$ | $-31 \pm 1$ | $28 \pm 10$ | $98 \pm 10$ | 3 |

[a] The binding enthalpy was determined directly from the ITC titration curves. From these experimentally determined parameters, the free energy of binding ($\Delta G$) and the entropy change ($\Delta S$) are obtained using the standard thermodynamic relationship $\Delta G = -RT \ln K = \Delta H - T\Delta S$. The experiments were performed $n$ times, and average values are given as well as standard deviations.

to associate with the LAH4 peptide only slightly exceeds the level of charge neutrality, in excellent agreement with the small positive $\zeta$ potential (*52*).

This peptide load decreases by about half when the pH is lowered to 5.5 (Figure 6). The thermodynamic signature, encompassing both significant entropic and enthalpic contributions (Table 1), suggests that electrostatic and other interactions, such as hydrophobic and van der Waals, contribute (*25*, *54*). This is probably due to a closer association of the remaining peptides with DNA. We have also performed experiments where the complexes were formed at neutral pH and the release of peptide was measured when the pH decreases (Figure 6). This approach tests that peptide association is indeed reversible and at the same time provides a closer match to the processes that occur in the endosome.

In comparison to polypeptides that bind to specific DNA sequences (e.g., refs *22* and *50*), the results shown here indicate that a very high molar ratio of LAH4 is required to saturate the binding sites of DNA. The high density of peptides on the DNA double helix (Figure 6) seems clearly too large to account for a tight and specific interaction of all peptides or to correlate with a model where the helix is well-inserted within the major groove of the DNA. Instead, one could imagine that several layers of peptides reside around the DNA, possibly by interacting with each other through their hydrophobic surfaces. Alternatively, a high density of peptides can be created by end-on association of the peptides with the DNA double helix. In this case, one charged peptide terminus is in contact with the DNA, whereas the other one is oriented away from the double helix. In both models, the DNA is covered by peptides exposing a positively charged surface. These charges are available for interactions with neighboring DNA strands, thereby condensing the elongated DNA double helix into large globular aggregates. The charged surface permits the complex to stay in suspension and helps association with negatively charged biomolecules, for example, at the cellular outer layers. Notably, DNA condensation has been demonstrated to be a critical feature for DNA stability and enhanced transfection efficiency (*20*). Clearly, although the above-mentioned models provide an explanation of how the high peptide density can be accommodated, experimental data, such as intermolecular distance measurement within the complexes acquired using solid-state NMR techniques, are required to understand the peptide−DNA interactions in detail.

The gel retardation data (Figure 5), the centrifugation assay (Figure 6), and the ITC studies (Figure 7) all indicate a high density of peptides on the DNA and a significantly decreased capacity of binding following acidification of the environment. This latter observation is easily explained by considering that, at pH 7.5, the LAH4 lysines and the N terminus

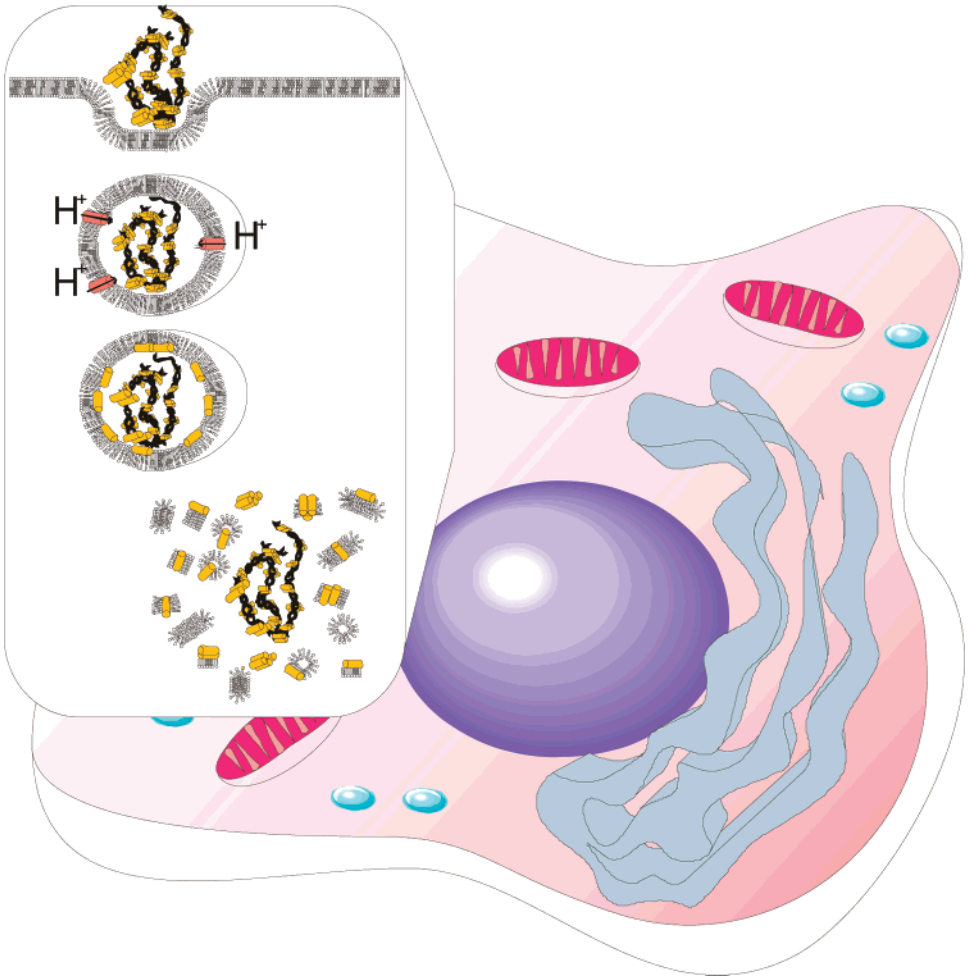


FIGURE 8: Mechanism of transfection of eukaryotic cells by the LAH4/DNA complexes. (a) Complex formation and compaction of the DNA molecules by interactions with LAH4, (b) endocytosis of the large LAH4/DNA complexes, (c) acidification of the endosome concomitant with the release of LAH4, (d) partitioning of the free LAH4 peptides into the membrane and lysis, (e) complex delivery to the cytoplasm and intracellular routing, transport to the nucleus, and expression. The image shows the following cellular compartments: nucleus (dark blue), endoplasmic reticulum and vesicles (gray), and mitochondria (dark pink). The enlargement to the top left shows the formation and disruption of endosomes carrying transfection complexes. The proton channels are shown in pink, and the LAH4 peptides are shown in yellow.

are the only positively charged amino acids, conferring a nominal charge of +5 to the peptide, whereas at pH 5.5, protonation of the histidines increases the peptide nominal charge to +9. More peptides are therefore required at neutral conditions before the negative charges on the DNA become saturated. Although the net charge of the complex does not change much during this process, these modifications in composition lead to structural alterations and a reduction in the solubility of the complex (Figure 3B).

A model summarizing the data is shown in Figure 8: The LAH4 peptides bind to DNA by nonspecific interactions, generating large complexes in the presence of salt. After cell binding, the LAH4/plasmid complexes enter the cell via an endosomal pathway (*15*). To achieve good transfection efficiency, the proton pumps of the endosome have to be active (*15*). The resulting drop in pH inside the endosome liberates a major fraction of peptides, which are free to interact with the endosomal membrane. Indeed, when "mutants" of LAH4 were investigated, the best transfection activities are observed for those peptides that change their membrane alignment from transmembrane to in-plane at about pH 6 (*15*), whereas peptides that exhibit a constitutively high amphipathic moment, e.g., by replacing the histidine residues by lysines, are much less active (*15*). Notably, doubling of the number of lysine residues at the termini results in a sharp drop in transfection efficiency (*52*), which can be explained by a reduction of the number of peptides released upon acidification.

A number of cationic, highly amphipathic peptides have been shown to be membrane-active and to efficiently partition into phospholipid bilayers (*16*, *55*). LAH4 has been demonstrated to exhibit membrane-partitioning constants in the $10^3-10^4$ $M^{-1}$ range for palmitoyloleoylphosphatidylcholine (POPC) or mixed zwitterionic/acidic liposomes, respectively (*16*), indicating good to high affinity also for the endosomal membranes. Considering the approximate geometries of the transfection complexes (*52*) and the endosomes, it is possible to estimate that the number of liberated peptides greatly exceeds the number of endosomal lipids. It has previously been shown that, at low pH, amphipathic helices, including peptides of the LAH4 family, preferentially associate with negatively charged lipids and cause significant disordering of their fatty acyl chain packing and this effect correlates with transfection efficiency (*56*, *57*). These data are therefore suggestive that the detergent-like amphipathic properties of LAH4 provoke openings in

or lysis of the endosomal membranes (*55*, *58*). With the disruption of the endosomal membrane, the peptide ensures access of the transfection complex to the cytoplasm.

With the model shown in Figure 8, three fundamental requirements can be defined for the design of new transfection molecules that use similar cellular pathways: First, complex formation by electrostatic interactions is a first requirement, easily accomplished by cationic functional groups. Second, the release of the molecules from the complex upon acidification requires titration of some of these groups, concomitant with a significant modification of the electrostatic interactions between neutral and acidic pH. Third, the liberated molecules should exert a detergent-like action on the endosomal membranes, i.e., adopt an amphipathic structure. Other processes, which are thus far much less well-understood, help in the transfer of DNA to the nucleus, where the genetic information is expressed.

## ACKNOWLEDGMENT

The 4 kbp salmon sperm DNA initially used was a kind gift from Dr. Bruno Senger, IBMC, Strasbourg, France. We are grateful to Dr. James Mason for proofreading the manuscript.

## REFERENCES

1. Anderson, W. F. (1998) Human gene therapy, *Nature 392*, 25−30.
2. Haensler, J., and Szoka, F. C., Jr. (1993) Synthesis and characterization of a trigalactosylated bisacridine compound to target DNA to hepatocytes, *Bioconjugate Chem. 4*, 85−93.
3. Michael, S. I., and Curiel, D. T. (1994) Strategies to achieve targeted gene delivery via the receptor-mediated endocytosis pathway, *Gene Ther. 1*, 223−232.
4. Boussif, O., Lezoualc'h, F., Zanta, M. A., Mergny, M. D., Scherman, D., Demeneix, B., and Behr, J. P. (1995) A versatile vector for gene and oligonucleotide transfer into cells in culture and in vivo: Polyethylenimine, *Proc. Natl. Acad. Sci. U.S.A. 92*, 7297−7301.
5. Ferrari, S., Moro, E., Pettenazzo, A., Behr, J. P., Zacchello, F., and Scarpa, M. (1997) ExGen 500 is an efficient vector for gene delivery to lung epithelial cells in vitro and in vivo, *Gene Ther. 4*, 1100−1106.
6. Wolfert, M. A., Schacht, E. H., Toncheva, V., Ulbrich, K., Nazarova, O., and Seymour, L. W. (1996) Characterization of vectors for gene therapy formed by self-assembly of DNA with synthetic block co-polymers, *Hum. Gene Ther. 7*, 2123−2133.
7. Gao, X., and Huang, L. (1995) Cationic liposome-mediated gene transfer, *Gene Ther. 2*, 710−722.
8. Behr, J. P. (1994) Gene transfer with synthetic cationic amphiphiles: Prospects for gene therapy, *Bioconjugate Chem. 5*, 382−389.
9. Wyman, T. B., Nicol, F., Zelphati, O., Scaria, P. V., Plank, C., and Szoka, F. C., Jr. (1997) Design, synthesis, and characterization of a cationic peptide that binds to nucleic acids and permeabilizes bilayers, *Biochemistry 36*, 3008−3017.
10. Fominaya, J., Gasset, M., Garcia, R., Roncal, F., Albar, J. P., and Bernad, A. (2000) An optimized amphiphilic cationic peptide as an efficient non-viral gene delivery vector, *J. Gene Med. 2*, 455−464.
11. Hart, S. L., Collins, L., Gustafsson, K., and Fabre, J. W. (1997) Integrin-mediated transfection with peptides containing arginine−glycine−aspartic acid domains, *Gene Ther. 4*, 1225−1230.
12. Midoux, P., Mendes, C., Legrand, A., Raimond, J., Mayer, R., Monsigny, M., and Roche, A. C. (1993) Specific gene transfer mediated by lactosylated poly-L-lysine into hepatoma cells, *Nucleic Acids Res. 21*, 871−878.
13. Plank, C., Oberhauser, B., Mechtler, K., Koch, C., and Wagner, E. (1994) The influence of endosome-disruptive peptides on gene transfer using synthetic virus-like gene transfer systems, *J. Biol. Chem. 269*, 12918−12924.
14. Zanta, M. A., Belguise-Valladier, P., and Behr, J. P. (1999) Gene delivery: A single nuclear localization signal peptide is sufficient to carry DNA to the cell nucleus, *Proc. Natl. Acad. Sci. U.S.A. 96*, 91−96.
15. Kichler, A., Leborgne, C., März, J., Danos, O., and Bechinger, B. (2003) Histidine-rich amphipathic peptide antibiotics promote efficient delivery of DNA into mammalian cells, *Proc. Natl. Acad. Sci. U.S.A. 100*, 1564−1568.
16. Vogt, T. C. B., and Bechinger, B. (1999) The interactions of histidine-containing amphipathic helical peptide antibiotics with lipid bilayers: The effects of charges and pH, *J. Biol. Chem. 274*, 29115−29121.
17. Bechinger, B. (1996) Towards membrane protein design: pH dependent topology of histidine-containing polypeptides, *J. Mol. Biol. 263*, 768−775.
18. Porcelli, F., Buck-Koehntop, B. A., Thennarasu, S., Ramamoorthy, A., and Veglia, G. (2006) Structures of the dimeric and monomeric variants of magainin antimicrobial peptides (MSI-78 and MSI-594) in micelles and bilayers, determined by NMR spectroscopy, *Biochemistry 45*, 5793−5799.
19. Henzler Wildman, K. A., Lee, D. K., and Ramamoorthy, A. (2003) Mechanism of lipid bilayer disruption by the human antimicrobial peptide, LL-37, *Biochemistry 42*, 6545−6558.
20. Bloomfield, V. A. (1996) DNA condensation, *Curr. Opin. Struct. Biol. 6*, 334−341.
21. Bechinger, B., Kinder, R., Helmle, M., Vogt, T. B., Harzer, U., and Schinzel, S. (1999) Peptide structural analysis by solid-state NMR spectroscopy, *Biopolymers 51*, 174−190.
22. Dragan, A. I., Klass, J., Read, C., Churchill, M. E., Crane-Robinson, C., and Privalov, P. L. (2003) DNA binding of a non-sequence-specific HMG-D protein is entropy driven with a substantial non-electrostatic contribution, *J. Mol. Biol. 331*, 795−813.
23. Keller, M., Tagawa, T., Preuss, M., and Miller, A. D. (2002) Biophysical characterization of the DNA binding and condensing properties of adenoviral core peptide $\mu$, *Biochemistry 41*, 652−659.
24. Lundbäck, T., Hansson, H., Knapp, S., Adenstein, R., and Härd, T. (1998) Thermodynamic characterization of non-sequence-specific DNA-binding to the Sso7d protein from *Sulfolobus solfataricus*, *J. Mol. Biol. 276*, 775−786.
25. Seelig, J. (1997) Titration calorimetry of lipid−peptide interactions, *Biochim. Biophys. Acta 1331*, 103−116.
26. Seelig, J. (2004) Thermodynamics of lipid−peptide interactions, *Biochim. Biophys. Acta 1666*, 40−50.
27. Lobo, B. A., Koe, G. S., Koe, J. G., and Middaugh, C. R. (2003) Thermodynamic analysis of binding and protonation in DOTAP/DOPE (1:1): DNA complexes using isothermal titration calorimetry, *Biophys. Chem. 104*, 67−78.
28. Pector, V., Backmann, J., Maes, D., Vandenbranden, M., and Ruysschaert, J. M. (2000) Biophysical and structural properties of DNA·di$C_{14}$-amidine complexes. Influence of the DNA/lipid ratio, *J. Biol. Chem. 275*, 29533−29538.
29. Silhol, M., Tyagi, M., Giacca, M., Lebleu, B., and Vives, E. (2002) Different mechanisms for cellular internalization of the HIV-1 Tat-derived cell penetrating peptide and recombinant proteins fused to Tat, *Eur. J. Biochem. 269*, 494−501.
30. Rittner, K., Benavente, A., Bompard-Sorlet, A., Heitz, F., Divita, G., Brasseur, R., and Jacobs, E. (2002) New basic membrane-destabilizing peptides for plasmid-based gene delivery in vitro and in vivo, *Mol. Ther. 5*, 104−114.
31. Coeytaux, E., Coulaud, D., Le Cam, E., Danos, O., and Kichler, A. (2003) The cationic amphipathic α-helix of HIV-1 viral protein R (Vpr) binds to nucleic acids, permeabilizes membranes, and efficiently transfects cells, *J. Biol. Chem. 278*, 18110−18116.
32. Kichler, A., Leborgne, C., Coeytaux, E., and Danos, O. (2001) Polyethylenimine-mediated gene delivery: A mechanistic study, *J. Gene Med. 3*, 135−144.
33. Pines, A., Gibby, M. G., and Waugh, J. S. (1973) Proton-enhanced NMR of dilute spins in solids, *J. Chem. Phys. 59*, 569−590.
34. Kricheldorf, H. R. M. D. (1983) $^{13}$C NMR cross polarization/magic angle spinning spectroscopic characterization of solid polypeptides, *Macromolecules 16*, 615−623.
35. Howarth, O. W., and Lilley, D. M. J. (1978) Carbon-13 of peptides and proteins, *Prog. NMR Spectrosc. 12*, 1−40.
36. Saito, H., and Ando, I. (1989) High-resolution solid-state NMR studies of synthetic and biological macromolecules, in *Annual Reports on NMR Spectroscopy* (Webb, E. A., Ed.) pp 209−290, Academic Press, New York.

37. LaPlante, S. R., and Borer, P. N. (2001) *Biophys. Chem. 90*, 219−232.
38. Sreerama, N., and Woody, R. W. (2000) Estimation of protein secondary structure from circular dichroism spectra: Comparison of CONTIN, SELCON, and CDSSTR methods with an expanded reference set, *Anal. Biochem.* 252−260.
39. Leventis, R., and Silvius, J. R. (1990) Interactions of mammalian cells with lipid dispersions containing novel metabolizable cationic amphiphiles, *Biochim. Biophys. Acta 1023*, 124−132.
40. Zou, S. M., Erbacher, P., Remy, J. S., and Behr, J. P. (2000) Systemic linear polyethylenimine (L-PEI)-mediated gene delivery in the mouse, *J. Gene Med. 2*, 128−134.
41. Coeytaux, E., Coulaud, D., Le Cam, E., Danos, O., and Kichler, A. (2003) The cationic amphipathic α-helix of HIV-1 viral protein R (Vpr) binds to nucleic acids, permeabilizes membranes, and efficiently transfects cells, *J. Biol. Chem. 278*, 18110−18116.
42. Lauterwein, J., Bosch, C., Brown, L. R., and Wüthrich, K. (1979) Physicochemical studies of the protein−lipid interactions in melittin-containing micelles, *Biochim. Biophys. Acta 556*, 244−264.
43. Terwilliger, T. C., and Eisenberg, D. (1982) The structure of melittin. I. Structure determination and partial refinement, *J. Biol. Chem. 257*, 6010−6015.
44. Oren, Z., Lerman, J. C., Gudmundsson, G. H., Agerberth, B., and Shai, Y. (1999) Structure and organization of the human antimicrobial peptide LL-37 in phospholipid membranes: Relevance to the molecular basis for its non-cell-selective activity, *Biochem. J. 341*, 501−513.
45. Luca, S., Filippov, D. V., van Boom, J. H., Oschkinat, H., de Groot, H. J., and Baldus, M. (2001) Secondary chemical shifts in immobilized peptides and proteins: A qualitative basis for structure refinement under magic angle spinning, *J. Biomol. NMR 20*, 325−331.
46. Cornilescu, G., Delaglio, F., and Bax, A. (1999) Protein backbone angle restraints from searching a database for chemical shift and sequence homology, *J Biomol. NMR 13*, 289−302.
47. Lee, D. K., and Ramamoorthy, A. (1999) Determination of the solid-state conformations of polyalanine using magic-angle spinning NMR spectroscopy, *J. Phys. Chem. 103*, 271−275.
48. Henzler Wildman, K. A., Lee, D. K., and Ramamoorthy, A. (2002) Determination of α-helix and *β*-sheet stability in the solid state: A solid-state NMR investigation of poly(L-alanine), *Biopolymers 64*, 246−254.
49. Leupin, W., Wagner, G., Denny, W. A., and Wuthrich, K. (1987) Assignment of the 13C nuclear magnetic resonance spectrum of a short DNA-duplex with $^1$H-detected two-dimensional heteronuclear correlation spectroscopy, *Nucleic Acids Res. 15*, 267−275.
50. Berger, C., Jelesarov, I., and Bosshard, H. R. (1996) Coupled folding and site-specific binding of the GCN4-bZIP transcription factor to the AP-1 and ATC/CREB DNA studied by microcalorimetry, *Biochemistry 35*, 14984−14991.
51. Cooper, A., Johnson, C. M., Lakey, J. H., and Nollmann, M. (2001) Heat does not come in different colours: Entropy−enthalpy compensation, free energy windows, quantum confinement, pressure perturbation calorimetry, solvation and the multiple causes of heat capacity effects in biomolecular interactions, *Biophys. Chem. 93*, 215−230.
52. Kichler, A., Leborgne, C., Danos, O., and Bechinger, B. (2007) Characterisation of gene transfer processes mediated by histidine-rich peptides, *J. Mol. Med. 85*, 191−201.
53. Wightman, L., Kircheis, R., Rossler, V., Carotta, S., Ruzicka, R., Kursa, M., and Wagner, E. (2001) Different behavior of branched and linear polyethylenimine for gene delivery in vitro and in vivo, *J. Gene Med. 3*, 362−372.
54. Leavitt, S., and Freire, E. (2001) Direct measurement of protein binding energetics by isothermal titration calorimetry 22, *Curr. Opin. Struct. Biol. 11*, 560−566.
55. Bechinger, B., and Lohner, K. (2006) Detergent-like action of linear cationic membrane-active antibiotic peptides, *Biochim. Biophys. Acta 1758*, 1529−1539.
56. Mason, A. J., Martinez, A., Glaubitz, C., Danos, O., Kichler, A., and Bechinger, B. (2005) The antibiotic and DNA transfecting peptide LAH4 selectively associates with, and disorders, anionic lipids in mixed membranes, *FASEB J. 20*, 320−322.
57. Mason, A. J., Husnal-Chotimah, I. N., Bertani, P., and Bechinger, B. (2006) A spectroscopic study of the membrane interaction of the antimicrobial peptide pleurocidin, *Mol. Membr. Biol. 23*, 185−194.
58. Bechinger, B. (2005) Detergent-like properties of magainin antibiotic peptides: A 31P solid-state NMR study, *Biochim. Biophys. Acta 1712*, 101−108.
59. Coeytaux, E., Coulaud, D., Le Cam, E., Danos, O., and Kichler, A. (2003) The cationic amphipathic α-helix of HIV-1 viral protein R (Vpr) binds to nucleic acids, permeabilizes membranes, and efficiently transfects cells, *J. Biol. Chem. 278*, 18110−18116.

BI700766J